International Journal of Concrete Structures and Materials
Vol.18, No.1E, pp.03~09, June 2006

Corrosion Evaluation of Epoxy-Coated Bars in Chloride Contaminated Concrete Using Linear Polarization Tests

Oan-Chul Choi,[1] Si-Young Jung,[2] and Young-Soo Park[2]

(Received December 10, 2004, and accepted May 26, 2006)

Abstract: Five slab specimens with predefined cracks are examined to evaluate the corrosion behavior of epoxy-coated bars in chloride contaminated concrete, using linear polarization method. The test specimens were subjected to alternating weekly cycles of ponding in a salt solution and drying for 48 weeks. Test results show that the current density of the specimen of normal steel bars becomes 0.715 $\mu A/cm^2$ indicating that the steel bars are in moderate or high corrosion condition. However, the corrosion rates of the specimens with damaged epoxy-coated bars are significantly below 0.1 $\mu A/cm^2$ and the bars appears to be in passive condition. The damaged epoxy-coated bars with a corrosion inhibitor of calcium nitrite showed a corrosion rate of 0.110 μm/year or 56 percents of the corrosion rate of damaged epoxy-coated specimen without such an inhibitor, 0.195 μm/year. However, the corrosion rates of specimens containing the other two corrosion inhibitors, a combination of amines and esters or mixtures of organic alkenyl dicarboxyl acid salts are quite equivalent to the control specimen. The research technique of linear polarization resistance method has proven itself to be useful in measuring corrosion rates of reinforcement in concrete.

Keywords: epoxy-coated bars, corrosion rate, linear polarization test.

1. Introduction

Corrosion of steel bars in concrete is caused by the breakdown of the natural passivity when reinforcing steel bars are surrounded by highly alkaline pore water in the cement matrix. Chloride corrosion is a direct attack upon the passive layer. Iron dissolves in the pore water at the anode forming ferrous reinforcing steel to the cathode where they react with water and oxygen forming ferrous ions. The ferrous ions then go on to react further with oxygen and water to form solid corrosion products.[1-3]

Epoxy-coated steel bar are one of the main corrosion protection systems used in modern bridges. Coating creates a barrier to the chloride ions and electrically isolates the steel. However, if the coating is broken, the steel will begin to corrode. Any bare spots or "holiday" existing in the epoxy may become hot spots for accelerated corrosion.[4] McDonald et al.[5] used the Southern Exposure test to evaluate epoxy-coated steel bars reinforcing the concrete. A good correlation was observed in the mat-to-mat resistance, and the results obtained from the tests were confirmed through linear polarization and AC impedance tests.[5]

There is no single method for accurately measuring the corrosion of reinforcing bars in concrete. The measurement of half cell potentials is a quick method of defining areas of corrosion. It measures the electrochemical potential difference between anodic and cathodic areas by comparison with a standard reference cell. ASTM C 876[6] is used to evaluate the corrosion potential of reinforcing steel in concrete (Table 1). However, the half cell cannot be used to measure the rate of corrosion. It is used to plot isopotential maps that show the most anodic areas of steel.

The actual corrosion process is electrochemical. There are several methods of measuring the true, instantaneous rate of corrosion, and many of these are electrochemical methods.[1,7,9] They rely on measuring changes in the half cell potential as it is induced and use an electrochemical theory to calculate the corrosion current, ie. the rate of corrosion. This paper briefly introduces the technique of linear polarization and describes the test results to evaluate corrosion behavior of epoxy-coated steel bars used in reinforced concrete structures.

2. Linear polarization resistance test and corrosion rate

2.1 Overview of linear polarization test

For reinforcing steel, iron is oxidized at the anode, causing ferrous ions to go into solution, and releasing electrons. This reaction can be

Table 1 Interpretation of half cell readings (ASTM C 876).

Half-cell reading (V)		Interpretation
CSE	SCE	
> −0.200	> 0.125	Greater than 90% probability that corrosion is not occurring
−0.200 to −0.350	−0.125 to −0.275	Corrosion activity is uncertain
< −0.350	< −0.275	Greater than 90% probability that corrosion is occurring

CSE: copper-copper sulfate electrode, SCE: saturated calomel electrode

[1] KCI member, School of Architecture, Soongsil University, Seoul 156-743, Korea. *E-mail: occhoi@ssu.ac.kr*
[2] KCI member, School of Architecture, Soongsil University, Seoul 156-743, Korea.

separated into two chemical equations as follows.

$$Fe \rightarrow Fe^{2} + 2e^{-} \text{ anodic reaction} \quad (1)$$

$$2H^{+} + 2e^{-} \rightarrow H_2 \text{ cathodic reaction} \quad (2)$$

Electrochemical reactions such as Eq. (1) and Eq. (2) proceed only at a finite rate. If electrons are made available as in the right side of Eq. (2), the potential at the surface becomes more negative, suggesting that excess electrons with their negative charges accumulate at the metal/solution interface waiting for reaction. That is, the reaction is not fast enough to accommodate all available electrons. This negative potential change is called cathodic polarization. Similarly, a deficiency of electrons in the metal liberated by Eq. (1) at the interface produces a positive potential change called anodic polarization. As the deficiency becomes greater, the tendency for anodic dissolution becomes greater. Anodic polarization represents a driving force for corrosion by the anodic reaction. When surface potential measures more positive, the corrosive power of the solution increases because the anodic polarization is greater.

In an aqueous electrolyte solution, the surface will reach a steady state potential, E_{corr}, which depends on the rate at which electrons can be exchanged by the available cathodic and anodic reactions. As the surface potential increases above E_{corr} to E, the anodic rate or corrosion rate generally increases as shown schematically in Fig. 1. Anodic polarization is defined as $\varepsilon_a = E - E_{corr}$. In the absence of polarization, even the slightest driving force would produce very high rates, and the line in Fig. 1 would be horizontal with a zero slope.

The corrosion current density can be determined by the concept of reaction rates and polarization of electrochemical reactions at metal surface discussed above. Polarization resistance is used to determine the microcell corrosion rate of a metal. A potentiostat is used to impose a range of potentials on the metal usually −10 to + 10 mV versus the open circuit corrosion potential and measures the corresponding corrosion current. A polarization curve as shown in Fig. 2 is obtained, and a portion of this curve is linear. The slope of the linear portion of the curve is called the polarization resistance and is proportional to the corrosion resistance of the metal.

The corrosion current density is given by the Stern-Geary relationship (Stern and Geary 1957):

$$I_c = \frac{B}{R_p} \quad (3)$$

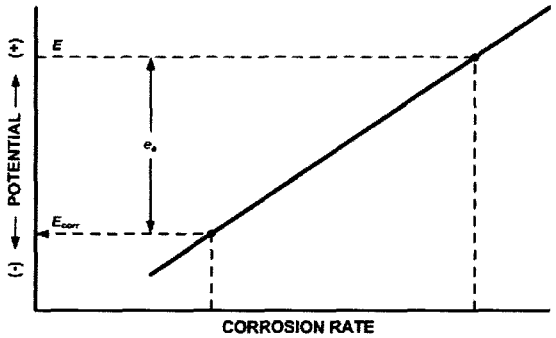

Fig. 1 Schematic increase in corrosion rate with increasing potential E and anodic polarization.[7]

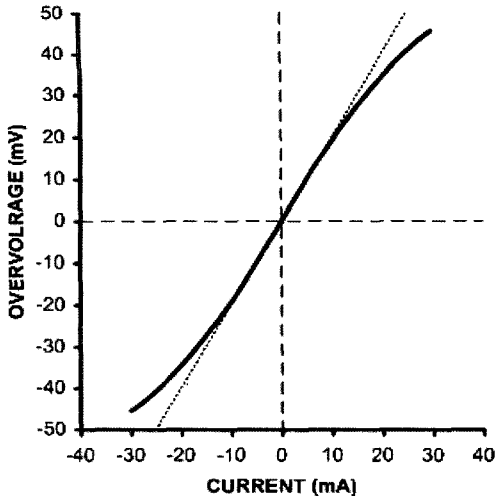

Fig. 2 Hypothetical polarization curve.[7]

2.2 Corrosion rate

Electrochemical reactions either produce or consume electrons. Thus, the rate of electron flow to or from a reacting interface is a measure of reaction rate. Electron flow is conveniently measured as current, I, in amperes, where 1-ampere is equal to 1-coulomb of charge (6.2×10^{18} electrons) per second. The proportionality between I and mass reacted, m, in an electrochemical reaction is given by Faraday's Law;

$$m = \frac{Ita}{nF} \quad (4)$$

Where F is Faraday's constant (96,500 coulombs/equivalent), n the number of equivalents exchanged, a the atomic weight, and t the time. Dividing Eq. (4) by t and the surface area, A, yields the corrosion rate, r;

$$r = \frac{m}{tA} = \frac{ia}{nF} \quad (5)$$

Where i, defined as current density, equals I/A. Eq. (5) shows a proportionality between mass loss per unit area per unit time (e.g., $mg/dm^2/day$) and current density (e.g., $\mu A/cm^2$). Thus, electrochemical measurements are very sensitive and convenient tools for the study of corrosion in the laboratory and the field.

The corrosion rate of a reinforcing bar subjected to a corrosion test, by which the corrosion current density is measured, can be obtained using Faraday's law, as shown in Eq. (4). The current density i can be obtained from a test where a macrocell has formed or from polarization resistance measurements, as explained below. The unit of penetration per unit time results from dividing Eq. (5) by the density, D, of the alloy. For corrosion rate in μm per year, Eq. (5) becomes

$$Corrosion\ rate = k\frac{ia}{nFD} \quad (6)$$

Where, the corrosion rate[7] is given in the unit dimension of μm/year.

3. Experimental program

3.1 General

Southern exposure specimens consist of small concrete slabs

containing two mats of steel. The slabs are subjected to alternating cycles of ponding in a salt solution and drying. The Southern Exposure test was originally developed by Pfeifer and Scali[11] to simulate the exposure conditions in southern climates, thus named Southern Exposure. A flexural crack was induced in the specimens to evaluate the behavior of cracked concrete. The cycle for these tests consisted of ponding the specimens for 100 hours in a 15 percent NaCl solution followed by drying in a heat chamber at 38°C for 68 hours. This weekly cycle was repeated 48 times.

3. 2 Materials

The materials tested include conventional uncoated reinforcing steel bars, epoxy-coated reinforcing steel bars and concrete without or containing corrosion inhibitors. D16 bars were used, and each bar was 305 mm long. Partially damaged epoxy-coated bars were used to evaluate the corrosion behavior. The epoxy coating was intentionally damaged by drilling four holes of 0.3 mm diameter through the coating on each epoxy-coated steel bar. In addition, the current study evaluated three corrosion inhibitors, DCI-S, Rheocrete 222+ and Hycrete DSS[10]. Concrete with water-cement ratio of 0.45 was used. The material composition and the number of test specimens are summarized in Table 2.

Darex Corrosion Inhibitor (DCI) is considered to be an anodic inhibitor since it works to minimize the anodic reaction by reacting with ferrous ions to form a γ-ferric oxide layer at the anode. DCI-S is composed of approximately 30% calcium nitrite and 70% water. Rheocrete 222+ is a combination of amines and esters in water. This inhibitor protects the reinforcing steel bars by forming a protective film on the steel surface and reducing the penetration of chloride ions into the concrete. Hycrete DSS consists of approximately 75% of water and 25% mixtures of organic alkenyl dicarboxylic acid salts and additives. The concrete mixing properties for each specimen is given in Table 3.

3. 3 Test specimens

The Southern Exposure test specimen is illustrated in Fig. 3.

Table 2 Test specimens.

Specimens designation	Steel designation*	w/c	Inhibitors
CB-4N-45N	Conv.	0.45	None
CB-ERC4-45N	ECR	0.45	None
CB-ERC-DCI	ECR-4h	0.45	DCI-S
CB-ERC-HY	ECR-4h	0.45	Hycrete DSS
CB-ERC-RH	ECR-4h	0.45	Rheocrete 222+

*Conv. = conventional steel. ECR = normal epoxy-coated steel
4h = epoxy coated bar damaged by 4 drill holes of 0.3mm diameter

The specimen consists of six reinforcing bars embedded in a concrete slab with a length of 305 mm, a width of 305 mm and a height of 178 mm. Two reinforcing bars as the top mat were placed with a clear cover of 25 mm and the bottom mat consists of four bars. The bars were drilled and tapped at both ends so that bolts can be fixed in molds to provide an electrical connection to the bars during tests. The top mat and bottom mats were connected to separate biding posts. The posts were connected by 10 Ω resistors. A dam was cast around the top surface of the specimen to facilitate ponding during the test. For the cracked slab specimens, a slot was cut at the bottom of the slab and a 3.2 mm and 300 mm long stainless steel shim was inserted to produce a simulated crack to the steel surface. Between 8 and 10 hours after casting, the stainless steel shim was removed, and a uniform crack was created in the slab.

3. 4 Polarization resistance test procedures

Polarization resistance tests were used to obtain the microcell corrosion rates of the specimens. The tests involved taking cell current readings in a short, slow sweep of the potentials. The sweep was typically from −20 to +20 mV relative to open circuit potential E_{oc}. In this range, the current versus voltage curve is roughly linear. A linear fit of the data to a standard model gives an estimate of the polarization resistance R_p, which can be used to calculate the corrosion density, I_{corr}, and corrosion rate. The tests were performed using a PC4/750 Potentiostat and DC105 corrosion measurement system purchased from Gamry Instruments.[13] The top mats of the specimens were used as the working electrode (WE) while the standard calomel was used as the reference electrode (REF). A thin plate of platinum was used as the counter electrode. The corrosion cell setup is shown in Fig. 4. The reinforcing bar

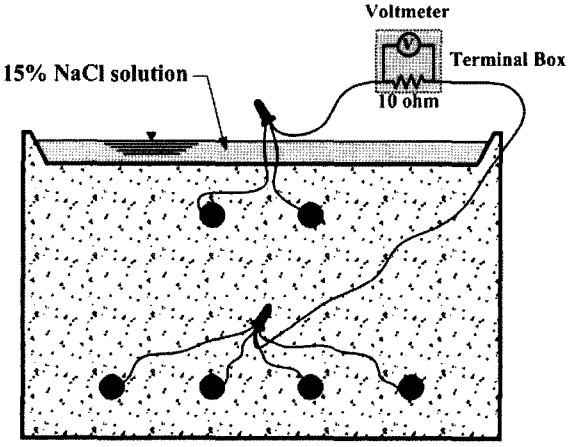

Fig. 3 A schematic diagram of a typical concrete test specimen

Table 3 Concrete mix proportions.

Water (kgf/m^3)	Cement (kgf/m^3)	CA (kgf/m^3)	FA (kgf/m^3)	AE (mL/m^3)	Rheocrete (mL/m^3)	DCI-S (mL/m^3)	Hycrete (kgf/m^3)
160	355	874	852	90	-	-	-
156	355	874	852	320	5000	-	-
147	355	874	852	140	-	15000	-
154	355	874	852	35	-	-	8

Inhibitor dosage rate
Rheocrete 222+5L/m^3, DCI-S : 15K/m^3, Hycrete : 2.25% of cement

(working electrode) was given a higher potential, and the corrosion rate was controlled by varying the current density appplied.

The assumed Tafel slopes (both anodic and cathodic) for corrosion of steel bars in concrete were typically 0.120 V, yielding a Tafer constant of $B = 26$ mV. The sample area of the rebar (defined as the surface area of the sample exposed to the solution) was 30,400 mm^2. The density and equivalent weight (atomic weight of an element divided by its valence) of steel bars were given as 0.0787 gf/mm^2 and 27.92, respectively. Compensation for resistance errors, R_s (a component of the electrolyte solution resistance), of the concrete specimen was optional.

Polarization experiments were performed at a scan rate of < 0.125 mV/s (ASTM G59 recommends a scan rate of < 0.1667 mV/s). The duration of the test was between 6 and 7minutes. Tests were performed on each specimen with at least 15 minutes of break between consecutive tests on the sample to allow the reinforcing bars to depolarize.

The data file from the polarization resistance test was analyzed by the Polres data analysis package provided with the DC 105. The user sets a graph scale to a full curve, a selected region, a frame, or chosen values and then picks a range of region in the graph for the analysis. The software uses a linear fit of data in the selected range to determine the polarization resistance. Then, the polarization resistance is used to determine the corrosion current density and corrosion rate. Fig. 5 shows the test setup for obtaining the linear polarization in this experimental design.

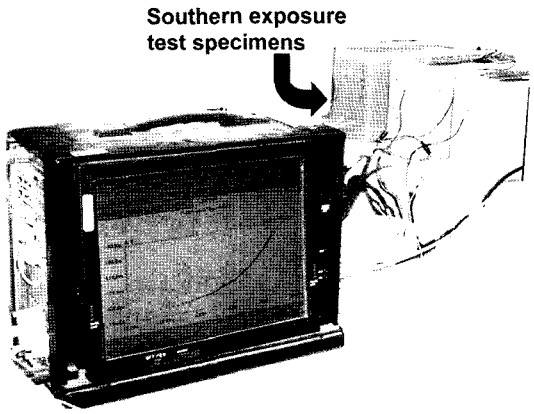

Fig. 5 Linear polarization test setup.

4. Test results and discussion

4.1 Polarization behavior

Fig. 6 shows polarization curves (voltage versus current density) of the specimens. The curve segment is used to calculate the corrosion rate. The R_p of the specimen is the slope of the polarization curve between the potential where the current equals zero, and is indicated here as the true open circuit potential, and the potential at +5mV above open circuit. The polarization curve in the vicinity of E_{corr} is linear only for a number of limited cases. The error occurs in magnitude and sign for the anodic and the cathodic test. The sources of error in measurements include 1) uncertainty in the Stern-Geary constant, B, 2) choice of a scan rate that is too fast, 3) neglecting the solution resistance, and 4) nonlinearity. The determination of β_a and β_c using available methods is difficult and sometimes even impossible. The value of the constant, $B = 26$ mV, used for the active corrosion of steel bars in concrete is appropriate, but the value of, $B = 52$ mV, for the passive state would give an estimate of the corrosion density with a better degree of accuracy. When combined with the polarization currents, the solution resistance for the concrete specimen produces an IR drop. Since we did not account for this resistance, we overestimated the polarization resistance and consequently underestimated the corrosion rate. Overall, the liner polarization resistance technique has proven itself to be useful in measuring corrosion rates of concrete reinforcement. It is also the most commonly used technique on account of its simplicity.

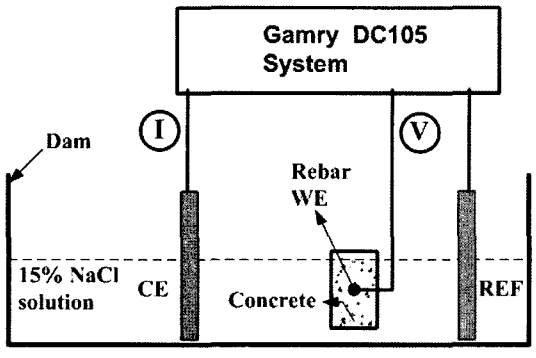

Fig. 4 Corrosion control cell by anodic polarization.

4.2 Corrosion rate evaluation

The guideline for estimating the corrosion rate from measured current density in reinforced concrete is summarized in Table 4. Cracking can occur at 10-100 mm/year depending on geometry, concrete quality, and oxygen access. This correlates well with the transition from moderate to high corrosion state. Rodriguez et al.[15] found that cracking due to corrosion occurs when the section loss is in the range of 10-30 μm/year for cover/rebar diameter ratios of 1 to 3. This interpretation assumed uniform corrosion. In the case of localized pitting, corrosion rates could be 5-10 times the general corrosion rate. Corrosion rate measurements are affected by temperature and relative humidity. Thus, the conditions of measurement will affect the interpretation and the boundary limits.

R_p is the most relevant parameter since it represents the corrosion resistance of the reinforcing bars. It can be used to evaluate the corrosion rate by applying Eq. (6), the Stern-Geary equation. A large R_p represents a high corrosion resistance. From Eq. (6), the corrosion current density, I_c, of each specimen is calculated. The corrosion rate is computed using Eq. (3), and the values are listed in Table 5. Values of R_p, I_{corr}, and corrosion rate are presented for all the specimens. It is evident from the results that the corrosion parameters of the reinforcing steel manifest the usual expected pattern in accordance with the likelihood of active corrosion of the five different slab specimens.

4. 3 Evaluation of epoxy-coated bars

Test results in this study show that the current density of normal steel-concrete specimen is 0.715 $\mu A/cm^2$ which means the steel bars are in moderate or high corrosion state based on the criteria for corrosion rate of reinforcing steel in concrete (Table 4). Furthermore, since the corrosion rate of the normal steel-concrete

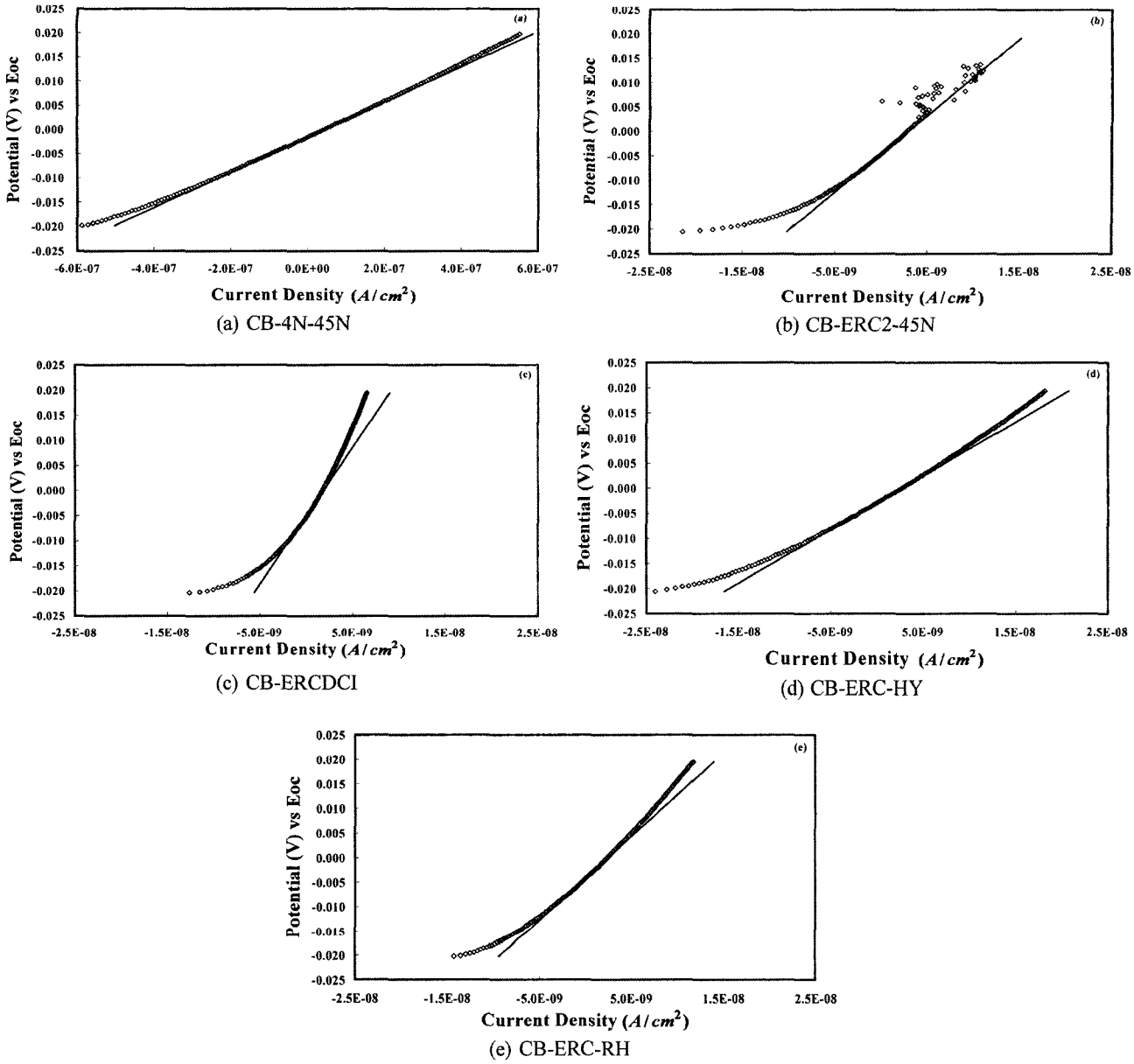

Fig. 6 Plots of potential vs. current density from polarization test results.

specimen was very high at 8.28 μm/year, cracking due to corrosion may occur in the specimen. However, the specimens with epoxy coated bars showed that the current densities were below 0.1 μA/cm^2 and they were in a passive (dormant) state for corrosion as illustrated in Fig. 7.

Corrosion rates for the epoxy-coated bars were calculated based on both the exposed area of the four 3.2 mm diameter holes drilled in the epoxy and the total area of the bars exposed to the salt solution. As for the exposed area of steel, the corrosion rate reached the value of 19.5 μm/year. The corrosion rate for the case of total bar area exposed to the solution was below that of normal steel. The epoxy-coated bars showed a corrosion rate of 0.195 μm/year based on the total area exposed to the solution or 2.4 percent of the corrosion rate of conventional (normal) steel, 8.28 μm/year. This finding allows us to conclude that epoxy-coated bars with minor damage performed much better than any normal uncoated reinforcing bars in the environment of chloride solution. The corrosion rates of specimens with epoxy-coated steel differed slightly depending on the corrosion inhibitors used.

Table 4 Criteria for corrosion rate of steel bars in concrete.

Corrosion rate (μA/cm^2)	Corrosion condition
$I_{corr} < 0.1$	Passive state
$0.1 < I_{corr} < 0.5$	Low to moderate corrosion
$0.5 < I_{corr} < 1.0$	Moderate to high corrosion
$1.0 < I_{corr}$	High corrosion

Table 5 Test results from linear polarization.

Specimens	E_{oc} (mV)	R_p (ohm cm^2×10^6)	I_{corr} (μA/cm^2)	Corrosion rate (μm/year)
CB -4N-45N	−485.0	0.036	0.715	8.28
CB-ERC4-45N	−600.0	1.57	0.0168	0.195
CB-ERC-DCI	−490.0	2.72	0.0096	0.110
CB-ERC-HY	−533.0	1.08	0.0244	0.283
CB-ERC-RH	−345.0	1.70	0.0154	0.178

4. 4 Effectiveness of corrosion inhibitors

To compare the effectiveness of corrosion inhibitors, the epoxy-coated rebar specimen without a corrosion inhibitor was used as the control specimen for this comparison analysis. The conventional (normal) steel bar specimen was excluded in this comparison. Table 5 shows the corrosion rates for specimens with different inhibitors. The corrosion rates of the reinforced concrete specimens with damaged epoxy-coated bars are much below 0.1 $\mu A/cm^2$ and the bars appears to be in passive state in terms of corrosion. The corrosion protection performance provided by calcium nitrite was definitely better than other three specimens as shown in Fig. 8. The epoxy-coated bars with calcium nitrite had a corrosion rate of 0.110 μm/year or 56 percent of the corrosion rate of the control specimen, 0.195 μm/year. It is known that nitrite ions compete with chloride ions for ferrous ions and react with ferrous ions to produce ferric oxide[2,12]. The corrosion rates of specimens containing amines and esters or mixtures of organic alkenyl dicarboxyl acid salts and additives were almost equivalent to the control specimen with no inhibitors. However, to Compare effectiveness of these corrosion inhibitors, the corrosion rates of control specimen should be in active corrosion state. A further study may elucidate the role of corrosion inhibitors more clearly and effectively in the future.

In studying the function of nitrites in inhibiting the corrosion of reinforcing steel in chloride environment in comparison to other inhibitors, the electrochemical techniques allows us to see the detail of the corrosion process. However, only the polarization resistance test allows us to obtain a quantitative value of the corrosion rate.

5. Conclusions

Based on the test results of specimens subjected to 48 weekly cycles of ponding in sodium chloride solution and drying, the following conclusions can be drawn.

1) The current density of normal steel bar specimen was 0.715 $\mu A/cm^2$, indicating that the uncoated steel bars were in moderate or high corrosion state. However, the corrosion rates of the concrete specimens reinforced with damaged epoxy coated bars were significantly below 0.1 $\mu A/cm^2$, and the bars appeared to be in passive state in terms of corrosion process. The epoxy-coated bars mixed with calcium nitrite had a corrosion rate of 0.110 m/year or 56 percent of the corrosion rate of damaged epoxy-coated specimen (control specimen) with no corrosion inhibitors, 0.195 m/year. The corrosion rates of specimens containing the other two corrosion inhibitors, a combination of amines and esters or mixtures of organic alkenyl dicarboxyl acid salts are quite equivalent with the control specimen. However, to compare effectiveness of these corrosion inhibitors, the corrosion rates of control specimen should be in active corrosion state.

2) Linear polarization method has proven itself useful in measuring corrosion rates of reinforcing steel bars in concrete.

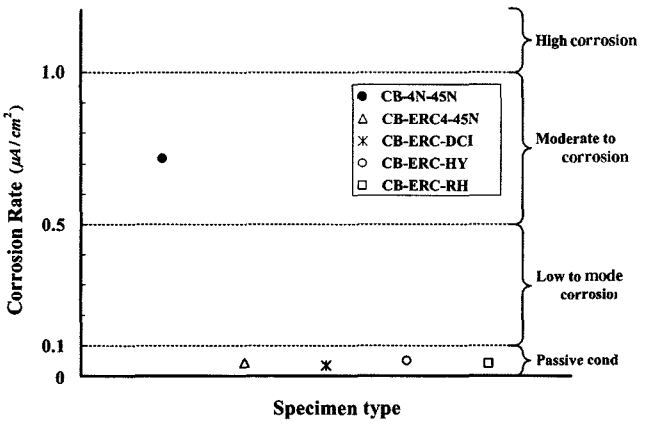

Fig. 7 Plot of corrosion rate vs. specimen type to determine corrosion conditions of the specimen.

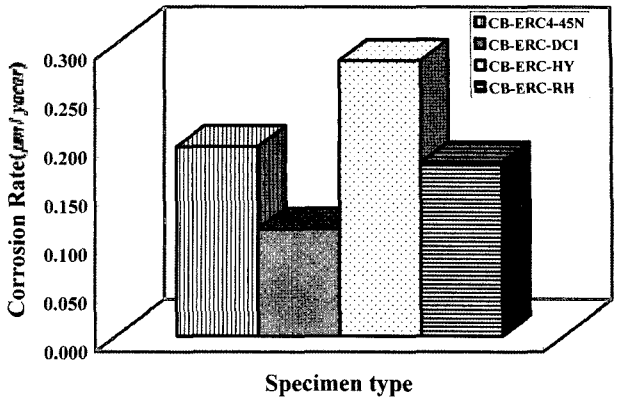

Fig. 8 Plot of corrosion rate vs. specimen type mixed with different inhibitors.

Acknowledgements

This work has been supported by the Soongsil University Research Fund. The financial support is gratefully acknowledged.

References

1. Uhlig, H. H. and Revie, W. R., *Corrosion and Corrosion Control, An Introduction to Corrosion Science and Engineering*, John Wiley & Sons, Inc, New York, 1985, 441pp.

2. Baidis, J. M. and Rosenberg, A. M., "The Inhibitors of Chloride-Induced Corrosion in Reinforced Concrete by Calcium Nitrite," *Cement, Concrete, Aggregates*, Vol.9 No.1, 1987, pp.30~33.

3. ASTM C 109-92a, *Standard Test Method for Determining the Effects of Chemical Admixtures on the Corrosion of Embedded Steel Reinforcement in Concrete Exposed to Chloride Environments*, 1994 Annual Book of ASTM Standards, Vol.4, No.2, American Society for Testing and Materials, West Conshohocken, PA, 1994, pp.113~119.

4. Lorentz, T. E., French, C. W. and Leon, R. T., *Corrosion of Coated and Uncoated Reinforcing Steel in Concrete*, Structural Engineering Report No. 92-03, University of Minnesota Center of Transportation Studies, 1992, 204pp.

5. McDonald, D. B., Pfeifer, D. W. and Sherman, M. R., *Corrosion Evaluation of a Epoxy-coated, Metallic-Clad and Solid Metallic Reinforcing Bars in Concrete*, Publication No. FHWA-RD-98-153, Federal Highway Administration, McLean, VA, 1998, 127pp.

6. ASTM C 876-91, *Standard Test Method for Half-Cell Poten-*

tials of Uncoated Reinforcing Steel in Concrete, 1994 Annual Book of ASTM Standards, Vol.4, No.2, American Society for Testing and Materials, West Conshohocken, PA, 1994, pp.432~437

7. Jones, D. A., *Principles and Prevention of Corrosion*, Macmillan Publishing Company, New York, NY, 1996, 572pp.

8. Berke, N. S., Shen, D. F. and Sundberg, K. M., *Comparison of the Polarization Resistance Technique to the Macrocell Corrosion Technique*, ASTM Special Technical Publication, Symposium on Corrosion Rates of Steel in Concrete, Baltimore, 1990, pp.38~51.

9. Hope, B. B., Page, J. A. and Ip, A. K. C., "Corrosion Rate of Steel in Concrete," *Cement and Concrete Research*, Vol.16, No.5, 1986, pp.771~786.

10. Balma, J., Darwin, D., Browning J. and Locke, C. E, *Evaluation of Corrosion Protection Systems and Corrosion Testing Methods for Reinforcing Steel in Concrete*, SM Report 05-1, The University of Kansas Center for Research, Inc., Lawrence KS, 2005, 517pp.

11. Pfeifer, D. W. and Scali, M. J., *Concrete Sealers for Protection of Bridge Structures*, National Cooperative Highway Research Board Program Report 244, Transportation Research Board, National Research Council, Washington, D.C., 1981, 138pp.

12. Zhang, J., Monterio, P. J. M. and Morrison H. F., "Non-invasive Surface Measurement of Corrosion Impedance of Reinforcing Bar in Concrete-Part 1: Experimental Results," *ACI Materials Journal*, Vol.98, No.2, March-April, 2001, pp.116~125.

13. Gamry, *Electrochemical Measurement System Software Installation Manuals*, Revision 3.1, Gamry Instruments Inc. 1999.

14. Allyn, M. and Franz G. C., "Corrosion Tests with Concrete Containing Salts of Alkenyl –Substituted Succinic Acid," *ACI Materials Journal*, Vol.98, No.3, May-June, 2001, pp.224~232.

15. Rodriguez, J, Ortega, L. M. Garcia, A. M. Johansson , L. and Peterson, K., "On Site Corrosion Rate Measurements in Concrete Structures Using a Device Developed under Eureka Project EU-401," *Proc. of International Conf. on Concrete Across Borders*, Vol.1, Odense, Denmark, June, 1994, pp.171~185.

Notation

a = atomic weight of the metal

$B = \dfrac{\beta_a \beta_c}{2.303(\beta_a + \beta_c)}$ = Stern-Geary constant, mV

D = density of the metal, g/cm^3

F = Faraday's constant (96,500 Coulombs/equivalent)

i = current density

I_c = corrosion current density, $\mu A/cm^3$

K = unit conversion factor = 31.5×10^4

n = number of ion equivalent exchanged

R_p = polarization resistance (slope of linear polarization curve), $k\Omega cm^2$